THE JOURNAL OF BIOLOGICAL CHEMISTRY VOL. 283, NO. 34, pp. 23048–23061, August 22, 2008
Printed in the U.S.A.

The Major Chemical-detoxifying System of UDP-glucuronosyltransferases Requires Regulated Phosphorylation Supported by Protein Kinase C*[S]

Received for publication, January 2, 2008, and in revised form, May 23, 2008 Published, JBC Papers in Press, June 13, 2008, DOI 10.1074/jbc.M800032200

Nikhil K. Basu[1], **Labanyamoy Kole**[1], **Mousumi Basu, Kushal Chakraborty, Partha S. Mitra, and Ida S. Owens**[2]
From the Heritable Disorders Branch, NICHD, National Institutes of Health, Bethesda, Maryland 20892-1830

Finding rapid, reversible down-regulation of human UDP-glucuronosyltransferases (UGTs) in LS180 cells following curcumin treatment led to the discovery that UGTs require phosphorylation. UGTs, distributed primarily in liver, kidney, and gastrointestinal tract, inactivate aromatic-like metabolites and a vast number of dietary and environmental chemicals, which reduces the risk of toxicities, mutagenesis, and carcinogenesis. Our aim here is to determine relevant kinases and mechanism(s) regulating phosphorylation of constitutive UGTs in LS180 cells and 10 different human UGT cDNA-transfected COS-1 systems. Time- and concentration-dependent inhibition of immunodetectable [^{33}P]orthophosphate in UGTs and protein kinase Cϵ (PKCϵ), following treatment of LS180 cells with curcumin or the PKC inhibitor calphostin-C, suggested UGT phosphorylation is supported by *active* PKC(s). Immunofluorescent and co-immunoprecipitation studies with UGT-transfected cells showed co-localization of UGT1A7His and PKCϵ and of UGT1A10His and PKCα or PKCδ. Inhibition of UGT activity by PKCϵ-specific antagonist peptide or by PKCϵ-targeted destruction with PKCϵ-specific small interference RNA and activation of curcumin-down-regulated UGTs with typical PKC agonists verified a central PKC role in glucuronidation. Moreover, *in vitro* phosphorylation of nascent UGT1A7His by PKCϵ confirms it is a *bona fide* PKC substrate. Finally, catalase or herbimycin-A inhibition of constitutive or hydrogen peroxide-*activated*-UGTs demonstrated that reactive oxygen species-related oxidants act as second messengers in maintaining constitutive PKC-dependent signaling evidently sustaining UGT phosphorylation and activity. Because cells use signal transduction collectively to detect and respond appropriately to environmental changes, this report, combined with our earlier demonstration that specific phospho-groups in UGT1A7 determined substrate selections, suggests regulated phosphorylation allows adaptations regarding differential phosphate utilization by UGTs to function efficiently.

Mammalian endoplasmic reticulum (ER)[3]-bound UDP-glucuronosyltransferase (UGT) isozymes carry out the broad and critical function of detoxifying endogenous and exogenous lipophilic phenols that include toxic metabolites, dietary constituents, environmental carcinogens, and, inadvertently, therapeutic agents. UGT isozymes inactivate a vast number of structurally diverse chemicals by attaching glucuronic acid to generate water-soluble products with high excretability. Because lipid solubility of chemicals taken into the body largely determines membrane permeability governing their absorption, distribution, and excretion, glucuronidation is the primary cellular process that protects against such chemicals (1). Chemicals are encountered on a regular basis due to their ubiquitous presence in dietary plants, pyrolysates of wood and petroleum products, distributions related to consumer and agricultural activities, and therapeutic agents. Critical endogenous substrates include bilirubin, steroids and their metabolites, bile acids, retinoic acids, thyroid hormones, and others (1). In the case of defective UGT$^{-/-}$, lipophiles accumulate in tissues leading to deleterious effects. Defective bilirubin-conjugating UGT1A1 (2) in Crigler-Najjar (*UGT1*$^{-/-}$) children causes elevated bilirubin levels that deposit in the central nervous system leading to kernicterus. Importantly, ingested dietary and environmental polyphenols are sometimes general toxins and genotoxins that can initiate cancer (3). To a detriment, glucuronidation converts medicinal chemicals, which lead to premature termination of therapeutic activity. Hence, it is essential to understand the mechanism(s) controlling this vital process.

Because individual recombinant UGTs are shown to have broad substrate activity toward aromatic-like chemicals (4), the 17 known viable members of the human superfamily of UGTs, distributed in families A, B, and C, collectively convert an unlimited number of chemicals. Because the ER-bound UGT isozymes have proven difficult to purify for tertiary structural analyses, the critical properties and mechanism(s) controlling catalytic activity are not understood. Whereas it has been demonstrated that UGT catalysis requires ongoing regulated phos-

* This work was supported, in whole or in part, by the National Institutes of Health NICHD Intramural Research Program. The costs of publication of this article were defrayed in part by the payment of page charges. This article must therefore be hereby marked "*advertisement*" in accordance with 18 U.S.C. Section 1734 solely to indicate this fact.

[S] The on-line version of this article (available at http://www.jbc.org) contains supplemental Figs. S1–S5.

[1] Both authors contributed equally to this work.

[2] To whom correspondence should be addressed: NICHD, National Institutes of Health, 9000 Rockville Pike, Bldg. 10, Rm. 9D-42, Bethesda, MD 20892-1830. Tel.: 301-496-6091; Fax: 301-480-8042; E-mail: owensi@mail.nih.gov.

[3] The abbreviations used are: ER, endoplasmic reticulum; UGT, UDP-glucuronosyltransferase; PKC, protein kinase C; DAG, 1,2-dihexanoyl-*sn*-glycerol; PMA, phorbol 12-myristate 13-acetate; PS, phosphatidylserine; MTT, 3-(4,5-dimethylthiazol-2-yl)-2,5-diphenyltetrazolium bromide; CE, common end; RACK, receptor for activated C-kinase; FITC, fluorescein isothiocyanate; TRITC, tetramethylrhodamine isothiocyanate; siRNA, small interference RNA; DAPI, 4′,6-diamidino-2-phenylindole; MOPS, 4-morpholinepropanesulfonic acid; CHAPS, 3-[(3-cholamidopropyl)dimethylammonio]-1-propanesulfonic acid; ROS, reactive oxygen species; MAP, mitogen-activated protein; EGF, epidermal growth factor.

phorylation (5–7), and that substrate selection may relate to phospho-group participation (7), it is critical to understand factors controlling the regulated phosphorylation.

Moreover, high concentrations of certain oxidizable flavonoids and polyphenols found in the diet are or become inhibitors of critical enzymes (8, 9), which we have now shown to include UGTs (5–7). By contrast, low levels of such chemicals often serve as antioxidants and chemopreventive agents (10), demonstrating the importance of chemical homeostasis. Here we demonstrate the relevant kinases and mechanism(s) involved in the regulation of ongoing phosphorylation of UGTs mediated by PKC signal transduction, which accounts for UGTs vulnerability to high concentrations of antioxidants.

EXPERIMENTAL PROCEDURES

Materials—Human LS180 colon and COS-1 cells were from ATCC (Manassas, VA). Tissue culture medium was from Cellgro (Rockville, MD), and serum was from Intergen (Purchase, NY). UGT substrates, curcumin, calphostin-C, calyculin-A, 1,2-dihexanoyl-*sn*-glycerol (DAG), phorbol 12-myristate 13-acetate (PMA), and phosphatidylserine (PS), kinase inhibitors, the MTT kit, catalase, and herbimycin-A were from either Sigma or Calbiochem; [^{14}C]UDP-glucuronic acid was from PerkinElmer Life Sciences. PKCϵ translocation activator and inhibitor peptides were from Calbiochem or Dr. D. Mochly-Rosen (Stanford University). Monoclonal anti-β-COP (ϵ-RACK) was from Sigma; anti-His was from Amersham Biosciences; and antibodies toward phosphoserine and protein kinase C isozymes were from Upstate Biotechnology (Lake Placid, NY) or Calbiochem. Donkey secondary antibodies conjugated with FITC or TRITC were from Jackson ImmunoResearch Laboratories (West Grove, PA). The immunogenic phospho-group in PKCϵ is 729 (Upstate, cat. #06-821). PKCϵ-specific siRNA (ON TARGET plus SMART Pool, Human PRKCE), and its non-targeting siRNA control were from Dharmacon (Chicago, IL). TnT® T7 Coupled Wheat Germ extract system was from Promega (Madison, WI). Rabbit anti-calnexin and rabbit anti-calreticulin were from Stressgen Biotechnologies (Victoria, Canada). The rabbit UGT1A-common end (CE) (11) and goat UGT-1168 antibodies have been described (12). pSVL-based constructs containing UGT1A1 (2), UGT1A3 (6), UGT1A4 (2), UGT1A6 (13), UGT1A7-10 (4), UGT2B7 (12), or UGT1B15 (14) were cloned or custom synthesized.

Growth and Transfection of Cells—LS180 colon and COS-1 cells were grown in Dulbecco's modified Eagle's medium with 10 and 4% fetal calf serum, respectively, and exposed to reagents solubilized in fresh Me_2SO diluted to $<0.5\%$. Cell viability was checked with a MTT kit after treatment with curcumin, calphostin-C, herbimycin-A, and other inhibitors as described in the text. Ten different pSVL-based UGT-cDNAs were transfected into COS-1 cells for specific protein expression as previously described (2). Also, His tag affinity ligand from the pcDNA3.1 vector (Invitrogen, Carlsbad, CA) was fused in-frame at the 3′-end of the cDNA in pSVL-UGT1A7 and pSVL-UGT1A10.

Glucuronidation Assay—Cellular extracts were analyzed for *in vitro* glucuronidation with abolition of UGT latency as previously described (15, 16). The common donor substrate, UDP-[^{14}C]glucuronic acid (1.4 mM, 1.4 μCi/μmol), was used in all reactions with unlabeled acceptor substrate. Incubations used 150 or 300 μg of cellular protein at pH 6.4 or 7.6 for 2 h at 37 °C (4), and glucuronides were separated by TLC. The product was quantified as previously described (15) using appropriate controls. Protein content was estimated using the BCA kit (Pierce), and it represents picomoles of glucuronide/mg of protein/per unit time.

Western Blot Analysis of UGTs and Protein Kinases in Cells—Relative amounts of UGT in transfected-COS-1 and LS180 cells were established by Western blot as previously established (5, 11). 25 μg of cellular homogenate were solubilized in SDS-sample buffer, applied to polyacrylamide (PAGE)-SDS gel and subjected to electrophoresis. Following protein electrotransblotting onto nitrocellulose membrane, regular blots were processed as previously described (11) for exposure to x-ray films. Membranes used with antibodies to target phospho-groups were blocked and processed as described (7). Blots were exposed to antibody specific for the *protein* of βII-, δ-, γ-, and ζ-PKC (not shown), of α- and ϵ-PKC, of MAP44/42 or to antibody specific for the *phosphate* group in PKCϵ (Ser-729), PKCα (Ser-657), or MAP44/42 according to supplier's instructions. Membranes were exposed to appropriate secondary antibody-horseradish peroxidase conjugate and visualized as described for anti-UGT.

In Situ Labeling of UGT and PKCϵ with [^{33}P]Orthophosphate—To determine whether UGTs undergo phosphorylation, LS180 cells were grown to nearly 100% confluency and processed as previously described (7, 17). All conditioned cells were exposed to [^{33}P]orthophosphate and to curcumin for 1–8 h to allow maximum inhibition and recovery or to calphostin-C for the final hour. Cells were harvested and solubilized; equal protein was allowed to immunocomplex with anti-UGT-CE, washed (12), and subjected to electrophoresis in a SDS-7.5% PAGE system. Similarly, solubilized cell extracts were immunocomplexed with anti-PKCϵ protein backbone, washed, and resolved by SDS-PAGE. Finally, the UGT-or PKCϵ-containing gel was fixed, dried, and scanned for quantitation as described for [^{14}C]glucuronides (15). Both gels were exposed to x-ray film.

Co-localization Studies—To determine whether UGT1A7His and *phospho*-PKCϵ co-localize, COS-1 cells, grown on Lab-Tek slides (Nalgene, Frederick, MD), were transfected (7) with pUGT1A7His. Cells were processed for immunofluorescence (7) by exposure to primary antibodies: rabbit anti-*phospho*(Ser-729)PKCϵ and mouse anti-His tag (Amersham Biosciences). *Phospho*-PKCϵ and 1A7His were visualized with donkey anti-rabbit-FITC conjugate and donkey anti-mouse-TRITC conjugate, respectively. Their images were assembled by computer using a photometric Zeiss microscope (Germany). For UGT1A10 and PKCα co-localization, rabbit anti-UGT-CE (4, 5, 11) and mouse anti-PKCα were added to UGT1A10His-transfected cells, and subsequently visualized with donkey anti-rabbit-FITC conjugate and donkey anti-mouse TRITC conjugate, respectively. For PKCδ and UGT1A10His co-localization, rabbit anti-PKCδ and mouse anti-His tag were added to UGT1A10His-transfected cells and subsequently visualized

with donkey anti-rabbit-FITC conjugate and donkey anti-mouse TRITC conjugate, respectively. All cells were exposed to DAPI fluorescein to identify nuclei.

Co-localization of PKCα and ER marker proteins, calnexin or calreticulin, in control cells was analyzed as follows: mouse anti-PKCα and rabbit anti-calnexin were added to cells and visualized with donkey anti-mouse TRITC and donkey anti-rabbit FITC conjugate, respectively. Also, co-localization of PKCα and calreticulin was determined by exposing cells to mouse anti- PKCα and rabbit anti-calreticulin and visualized with donkey anti-mouse TRITC conjugate and donkey anti-rabbit FITC conjugate, respectively.

Treatment of LS180 Cells with Agonists and Antagonists for PKCs—To show significant enzyme activation, we first inhibited cellular UGT activity with curcumin treatment before exposure to calyculin-A, DAG, PMA, or PS. Additionally, LS180 cells were treated with agonist or antagonist PKCϵ-specific peptide for different times as shown. For peptides lacking a cellular-permeating conjugate, cells were grown to confluency before permeabilizing with 45 μg/ml saponin (18). Permeabilized cells were exposed to medium containing octapeptide (Oct) represented in the V1 region of PKCϵ (19) or to its scrambled (Scr) control and allowed to uptake test peptide. A sequence also in the VI region of PKCϵ, Antennapedia-conjugated pseudo ϵ-RACK agonist peptide, was introduced into cells following curcumin pretreatment. Extracts of cells were assayed *in vitro*. (ϵ-RACK receptor is commonly known as β-COP (7, 19).)

Treatment of UGT1A7-transfected COS-1 Cells with PKCϵ-specific siRNA—PKCϵ-specific siRNA (100 nM) or its control (Dharmacon) was transfected according to the source's protocol into COS-1 cells, which had expressed UGT1A7His for 24 h; treatment continued for 48 h before harvesting cells for eugenol and mycophenolic acid (shown) glucuronidation as described above in 2-h incubations.

Co-immunoprecipitation Studies—COS-1 cells that expressed UGT1A7-, UGT1A10-, or each corresponding His construct were untreated or treated with curcumin or calphostin-C, harvested, solubilized in cold Kinexus lysis buffer (Kinexus, Vancouver, Canada) (modified Kinexus lysis buffer contained 20 mM MOPS buffer, pH 7.0, 2 mM EGTA, 5 mM EDTA, 30 mM NaF, 40 mM β-glycerophosphate, pH 3.2, 20 mM pyrophosphate, 1 mM sodium orthovanadate, 1 mM phenylmethysulfonyl fluoride, 3 mM benzamidine, 5 μM pepstatin, 10 μM leupeptin, 0.5% Nonidet P-40, and 5 mM CHAPS adjusted to pH 7.2), fractionated by centrifugation at 60,000 $\times$ *g* for 30 min, and subjected to co-immunoprecipitation as previously described using anti-UGT-CE or anti-His. Immunoprecipitates were resolved in SDS-PAGE gel systems and transblotted as described for Western blot analysis using antibodies given in respective figure legends.

In Vitro Transcription, Translation, and PKCϵ-dependent Phosphorylation of Nascent UGT1A7—The UGT1A7cDNA was inserted at the XbaI/BamH1 cloning site of pcDNA3.1 (−)/Myc-HisB (Invitrogen) downstream of the T7 RNA polymerase promoter followed by the polyadenylation consensus sequence; the construct was linearized by digesting with SmaI. Purified 1A7-containing construct was transcribed into mRNA, which was subsequently translated into UGT1A7Myc-His using a TnT^R T7 Coupled Wheat Germ extract system (Promega) that was incubated 90 min at 30 °C according to the manufacturer's protocol. To newly synthesized UGT1A7His, 10 ng of PKCϵ, 75 μM [γ-^{33}P]ATP (2.2 μCi/pmol), and other kinasing reactants (Upstate) were combined in 60 μl and allowed to react for 20 min at 30 °C according to the manufacturer's protocol. Aliquots (10 μl) of the reaction mixture were added to P81 cellulose membrane, washed with 0.75% phosphoric acid and acetone, air dried, and counted using a liquid scintillation system according to a Promega protocol. Also, the 250-μl reaction system was solubilized with an equal volume of 2$\times$ Kinexus buffer, centrifuged at 10,000 $\times$ *g* for 20 min, the supernatant was added to Ni^+-charged resin (Sigma), and the purification strategy followed the source's protocol. Duplicate 4–15% gradient SDS-PAGE systems were loaded with processed samples and electrophoresed; one gel was dried and exposed to x-ray film for development, and the duplicate gel was transblotted onto a nitrocellulose membrane and analyzed by Western blot as previously described using anti-His and anti-UGT-CE as already described.

Treatment of LS180 Cells with Catalase and Hydrogen Peroxide—To test effects of reactive oxygen species (ROS) on constitutive UGT activity, untreated LS180 cells were exposed to different concentrations of catalase or herbimycin-A. Also, cells were treated with different concentrations of H_2O_2 or combinations of H_2O_2 and catalase or herbimycin-A (20–23), or of H_2O_2 with curcumin or calphostin-C. Cellular extracts were tested for glucuronidation of eugenol and capsaicin (4).

RESULTS

Inhibition of UGTs Expressed in COS-1 and LS180 Cells by Curcumin or Calphostin-C Treatment—Our attempts to uncover special UGT properties associated with function began with a screen to discover new regulatory molecules among UGT substrates. While comparing in-cell treatment of two members, UGT1A7 and 1A10, of human UGT1A family that have similar properties, 1A7 was dramatically down-regulated by 200 μM curcumin, but 1A10 showed minor inhibition (Fig. 1*A*). With appropriate concentrations, there was rapid inhibition with recovery for all UGTs tested, re-exposure to curcumin caused the cycle to repeat for the three times tested (data not shown), suggesting the involvement of signaling events (24–28). As the substrate, curcumin, has been associated with antioxidant, anti-inflammatory, and anticarcinogenic effects in cells (24–26) and with inhibition of kinases (28), we tested other kinase inhibitors and found treatment with calphostin-C, a PKC-specific inhibitor (29), also rapidly down-regulated UGT, but without recovery (Fig. 1*A*). Interestingly, curcumin behaved as a typical substrate under *in vitro* conditions. Comparing equal protein amounts of UGT1A7 and 1A10 and increasing curcumin concentrations, saturation kinetics were observed with both isozymes (Fig. 1*B*), except 1A10 activity was approximately twice that of 1A7. Effects of curcumin treatment of ten independently expressed UGTs, UGT1A1, -1A3, -1A4, -1A6, -1A7 through -1A10, -2B7, and -2B15, in COS-1 cells showed that each was inhibited without affecting specific pro-

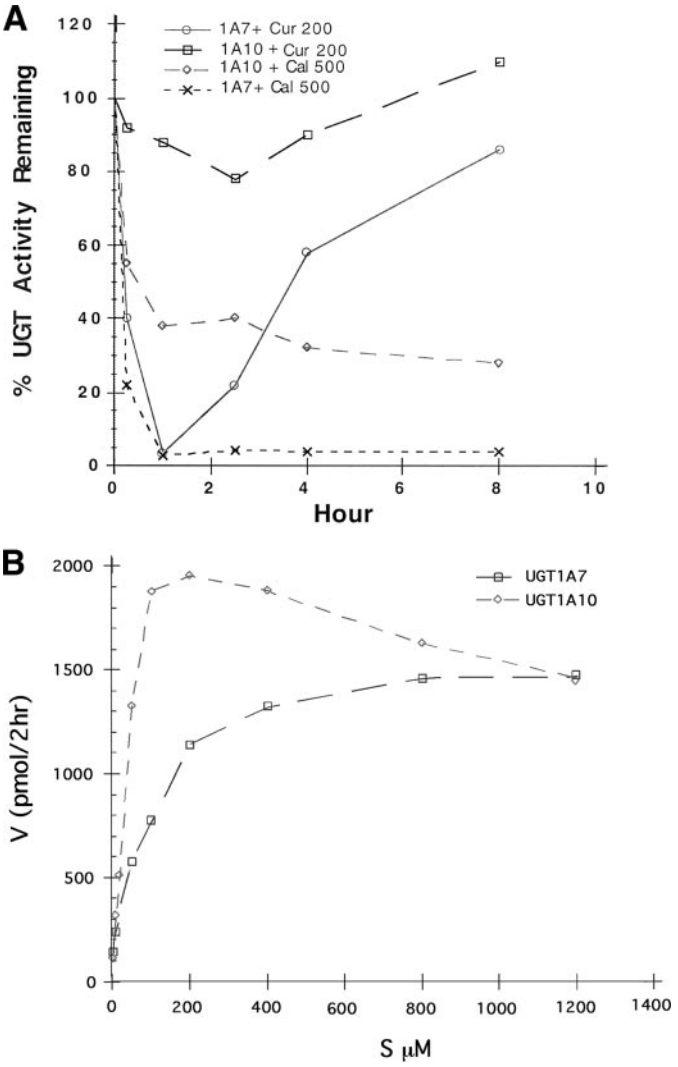

FIGURE 1. *A*, time course of human UGT1A7 or UGT1A10 activity expressed in COS-1 cells following treatment with curcumin and calphostin-C. Cells, untreated or treated with 200 μM curcumin or 500 nM calphostin-C as shown, were harvested; cell extracts were assayed *in vitro* as described under "Experimental Procedures." Experiments, carried out as described under "Experimental Procedures," were repeated thrice in triplicates; standard errors ranged from $\pm$2 to $\pm$5%. The MTT assay did not show toxicity after 8 h. *B*, *in vitro* glucuronidation of curcumin by UGT1A7 and UGT1A10 expressed in COS-1 cells using increasing concentrations. Experiments, carried out as described under "Experimental Procedures," were repeated thrice in triplicates; standard errors ranged from $\pm$2 to $\pm$3%.

tein (Fig. 2), and the inhibitory level of curcumin was isozyme-dependent (Fig. 2). Analysis of concentration dependence of curcumin and calphostin-C for two isozymes with contrasting characteristics (4, 7) showed UGT1A7 was among the most sensitive to the reagents, and UGT1A10 was the most resistant (supplemental Fig. S1). The concentration profiles for the eight other isozymes are not shown. Immunoprecipitates of UGT1A7 and -1A10 with anti-UGT-CE again (4, 6, 7, 11) showed there had been no effect on specific protein level, whereas immunoreactivity of anti-phosphoserine demonstrated (7) curcumin and calphostin-C caused concentration-dependent loss of phosphoserine in UGT1A7 and -1A10 (supplemental Fig. S1, *top*) with the former showing 2-fold greater sensitivity than the latter. These observations, including concentration-dependent inhibition of the 10 recombinant UGTs, led us to conclude that all UGT isozymes likely require phosphorylation that involves PKC isozymes. Moreover, predicted PKC phosphorylation sites by computer analysis have been identified in each of the 10 UGTs analyzed (5).

Antibodies to Different Kinases Distinguish the Effect of Curcumin on UGTs—Because several UGT isozymes are constitutively present in LS180 cells, we attempted to determine effect(s) of curcumin and calphostin-C on PKCs and UGT activities and their phosphorylation status. Because calphostin-C is a PKC-specific inhibitor, we initially examined its effect on LS180 cells by Western blot with antibodies against the *protein* backbone for α-, βII-, δ-, ϵ-, γ-, and ζ-PKC. After observing a change in profile for only PKCϵ following 50 μM curcumin treatment, we examined blots with anti-*phosphoserine*-729-PKCϵ and found the phospho-pattern (corrected with phospho-PKC/backbone PKC ratios) closely paralleled that for UGT activity (normalized with specific UGT levels shown in Fig. 3*A* (*panel 1*)). Proceeding from control through recovery, the ratios are: 1.07, 0.40, 0.10, 0.33, 0.60, 0.73, 0.92, and 0.98 (Adobe Photoshop, MACBas) and are compared with corresponding time points in the *bar graph* of Fig. 3*A* (*panel 4*). Although PKCϵ protein was maximally reduced at 1 h with little change between 2 and 6 h (Fig. 3*A*, *panel 2*), *phosphoserine-729*-PKCϵ was also maximally reduced at 1 h to non-detectable levels, but then more than doubled between 2 and 6 h with full recovery by 12 h (*panel 3*). Similar effects of curcumin on UGT activity and PKCϵ were seen in HT29 cells (data not shown).

By comparison, other kinases examined in LS180 cells were not affected by 50 μM curcumin treatment or showed an unrelated pattern. Reactivity of antibody toward the protein backbone or *phospho*-group of PKCα, like that for PKCβII, -δ, -γ, and -ζ (not shown), showed no detectable effect following 50 μM curcumin treatment (supplemental Fig. S2, *panels 3* and *4*). Further, immunoreactivity of anti-MAP44/42 kinase proteins was not altered by 50 μM curcumin (supplemental Fig. S2, *panel 1*), and immunoreactivity of anti-*phospho*-44/42 of MAP44/42 kinase was unrelated to the inhibitory profile of UGT (supplemental Fig. S2, *panel 2 versus* Fig. 3*A*, *panel 4*). Antibody to phospho-44 gave a progressive decrease in reactivity, and that toward phospho-42 gave a progressive increase. Although there was no detectable MAP44/42 kinase involvement, PD98059 (MEK (MAP kinase/extracellular signal-regulated kinase kinase) inhibitor) (10 μM) caused a modest 30% inhibition of UGT in 2 h. In addition, the calcium-channel blockers, nifedipine (500 nM, 20% inhibition) and TMB-8 (2.5 μM, 15% inhibition), or calmodulin antagonist, calmidazolium (1.0 μM, 16% inhibition), had little effect on UGT (data not shown). The dramatic loss of phosphate-729 in PKCϵ suggested curcumin, most likely, affected phosphorylation. Parallel loss of UGT activity and phospho-PKCϵ suggested this isozyme carried out one or more phosphorylation events critical for UGT(s) activity. Furthermore, inhibition of at least six different substrate activities tested with extracts of curcumin- and calphostin-C-treated LS180 cells and of similar extracts of COS-1 cells independently transfected with 8 *UGT1*-encoded cDNAs

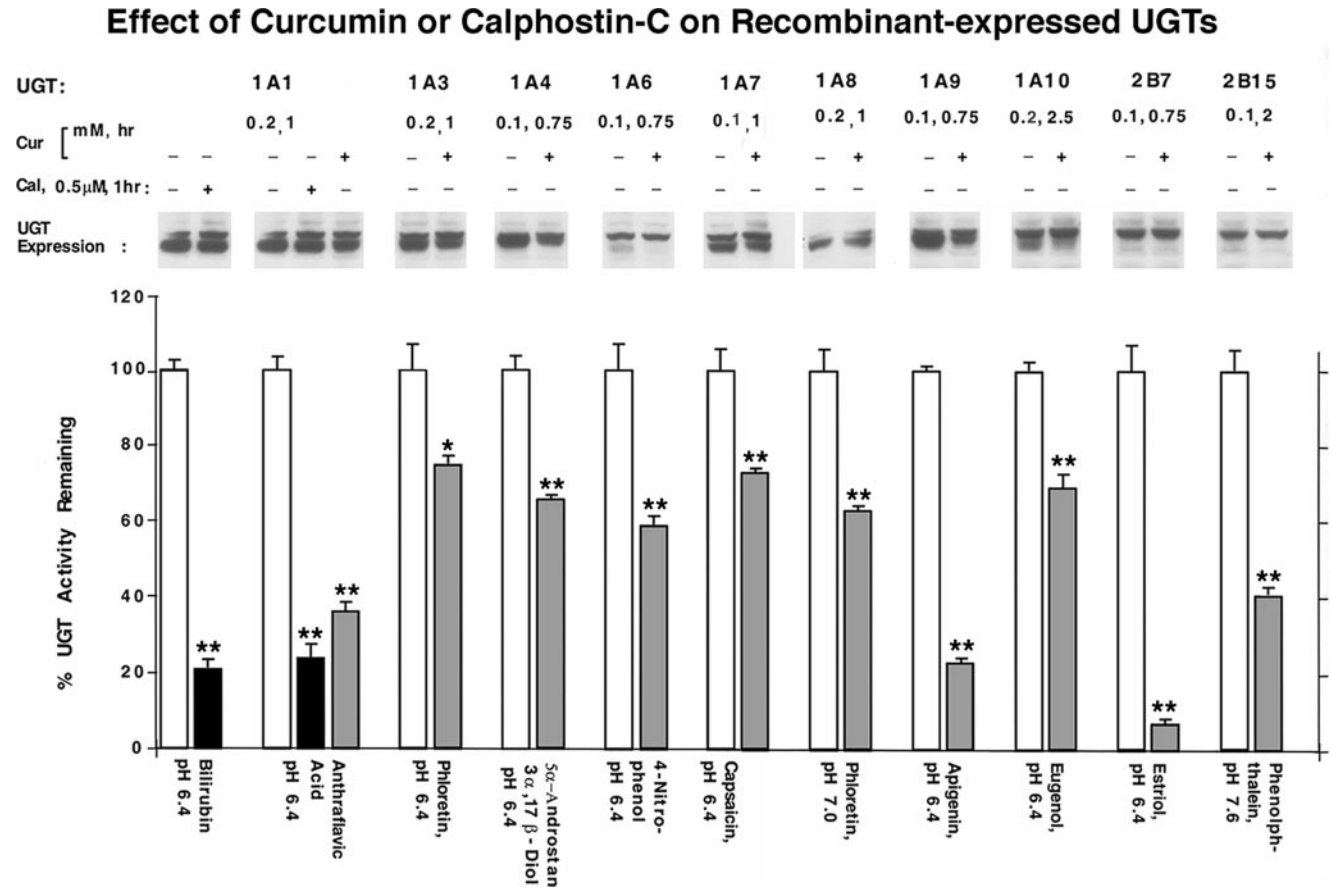

FIGURE 2. **Curcumin or calphostin-C treatment of UGT-transfected COS-1 cells.** 72 h after transfection with a pSVL-based UGT, COS-1 cells were treated with curcumin or calphostin-C; cell homogenates and substrates were as shown and used according to "Experimental Procedures." Homogenates were subjected to Western blot analysis with anti-UGT-CE (11) according to "Experimental Procedures." *, $p \leq 0.01$; **, $p \leq 0.001$.

and 2 *UGT2B*-encoded cDNAs (UGT2B7 and UGT2B15) (Fig. 2) indicates phosphorylation is likely required for all UGTs.

Fate of Curcumin during Reversal of Inhibition—To understand the reversal of inhibition, we determined the fate of 50 μM curcumin in LS180 cells. Combined results after the independent analysis of culture medium and of cell extract by high-performance liquid chromatography (30) showed that at 15 min there was 98.5% free curcumin and 1.5% curcumin-glucuronides; between 1 and 24 h free curcumin progressively decreased, and its glucuronides progressively increased (Table 1). A marked decrease in curcumin levels occurred between 2 and 3 h after treatment, which also compares to a significant increase in UGT activity (Fig. 3*A*, *panel 4*). Hence, recovery appeared to depend upon reduction of free curcumin to non-inhibitory levels by residual but progressively increasing UGT activity that simultaneously relieved PKCϵ inhibition. Importantly, UGT1A7- and -1A10-transfected cells, treated with 50 μM curcumin or 250 nM calphostin-C for 24 h and up to 400 μM curcumin or 1.0 μM calphostin-C for 3 h, did not show cell loss or toxicity by the MTT assay, which was similar to previous reports (21, 31, 32). Although results provide evidence that one or more kinase-dependent cycling events are required for UGT activity, reversal of curcumin inhibition is likely due to its glucuronidation by low UGT activity remaining that progressively increases with time.

Effect of Other PKC Inhibitors on UGT Activity—Also, treatment of LS180 cells with other PKC inhibitors at different concentrations decreased UGT activity (data not shown) within 15–120 min as follows: bisindolemaleimide (250 nM) by 40%, chelerythrine (2 μM) by 20%, Gö-6976 (1.0 μM) by 20%, and Ro-320432 (250 nM) by 30%. 10 μM bisindolemaleimide, chelerythrine, or Ro-320432 caused between 50 and 62% inhibition as seen earlier (7). Moreover, two phosphatidylinositol 3-kinase inhibitors, LY294002 (500 nM) and wortmannin (10 μM), caused 30–40% inhibition after 2 h. Also, we observed that UGT in LS180 cells, treated with 25 μg/ml cycloheximide, showed a modest 25% decrease in activity after 144 h, indicating a substantially long half-life and that loss of activity is unrelated to specific protein degradation (data not shown).

Incorporation of [^{33}P]Orthophosphate into UGTs and PKCϵ in LS180 Cells—Because curcumin and calphostin-C disruption of UGT activity in LS180 cells had no effect on UGT protein, suggesting that protein modification had occurred, we attempted to radiolabel UGTs with [^{33}P]orthophosphate and compare effects of curcumin and calphostin-C treatment. Isozymes in control cells were maximally labeled after 8-h exposure to orthophosphate as indicated by resolution of 52- and 55-kDa anti-UGT-CE immunoreactive bands in a SDS-7.5% PAGE system (Fig. 3*B*, *panel 4*, *lane 1*) compared with less resolved bands in the ECL-revealed Western blots of 15% gels

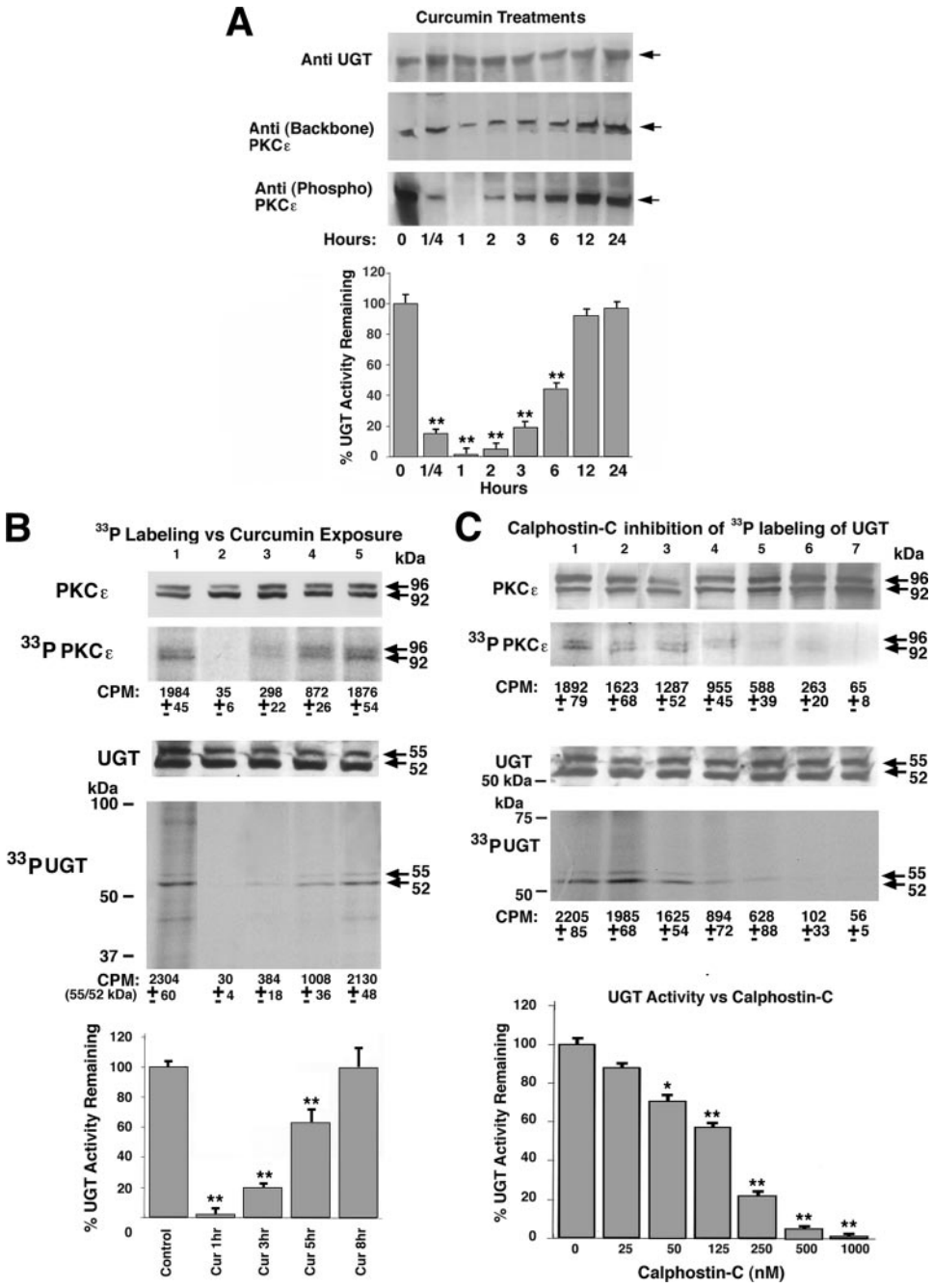

FIGURE 3. **Inhibition of UGT activity in LS180 cells by curcumin or calphostin-C treatment.** *A*, Western blot analysis of curcumin treated-cells used UGT and PKCϵ antibodies in parallel with glucuronidation activity. Extracts (25 μg of protein) from curcumin (50 μM)-treated or control cells were resolved in an SDS 4–15% PAGE system. Antibody toward UGT-CE (52–55 kDa), the protein backbone of PKCϵ (92–96 kDa), or phosphoserine-729-PKCϵ was added to separate Western blots and processed as described under "Experimental Procedures." *Panel 4* shows *in vitro* glucuronidation of capsaicin with control values of 1882 ± 96 pmol/mg of protein/h. Experiments were repeated more than five times. Standard errors for data range between ±1 and ±5%. **, $p \leq 0.001$. *B*, [^{33}P]orthophosphate labeling of both PKCϵ and UGT proteins with parallel inhibition of labeling and UGT activity following curcumin treatment of LS180 cells. All cells were exposed to [^{33}P]orthophosphate (5 mCi/ml) for 8 h and 50 μM curcumin for 0, 1, 3, 5, or 8 h as described under "Experimental Procedures." From solubilized cellular extract, immunocomplexes with anti-UGT-CE (*panel 4*) and with anti-PKCϵ (*panel 2*) were washed as described under "Experimental Procedures" before resolution on SDS-7.5% PAGE. Also, PKCϵ (*panel 1*) and UGT (*panel 3*) were analyzed by Western blots. Processed gels were exposed to x-ray film for 48 h. Experiments were repeated three times. UGT activity was toward capsaicin with control values of 1857 ± 74 pmol/mg of protein/h (*panel 5*); eugenol generated a similar profile (data not shown). *C*, concentration-dependent effects of calphostin-C on [^{33}P]orthophosphate incorporation into UGTs in LS180 cells. Cells were allowed to incorporate the label for 8 h with calphostin-C treatment over the final hour as described under "Experimental Procedures" before immunocomplexing and Western blotting as described under *C* (*panels 1–4*) and determining UGT activity toward capsaicin (*panel 5*). *, $p \leq 0.01$; **, $p \leq 0.001$.

(Fig. 3*A*, *top panel*). Additionally, [^{33}P]orthophosphate exposure in the presence of curcumin between 1 and 8 h showed maximum loss of label at 1 h (Fig. 3*B*, *panels 2* and *4*); compare label in 55/52-kDa bands with recovery by 8 h that paralleled UGT activity (*panel 5*) without effects on UGT protein (*panel 3*). PKCϵ radiolabeling (Fig. 3*B*, *panels 1* and *2*) parallels that for UGT. In addition, calphostin-C caused a concentration-dependent disruption of immunodetectable [^{33}P]-orthophosphate incorporation into the 52- and 55-kDa UGT proteins (*panel 4*) in parallel with down-regulated activity (Fig. 3*C*) without effects on UGT protein (*panel 3*). In summary, the two labeling studies with immunodetection of [^{33}P]PKCϵ and [^{33}P]UGT following curcumin and calphostin-C treatment revealed profiles similar to that seen with immunodetection of unlabeled UGTs in LS180 cells and to the two recombinant UGTs, respectively; compare the following: (*a*) CPM for [^{33}P]PKCϵ with those for [^{33}P]UGT (Fig. 3*B*, *panels 2* and *4*) to the data in Fig. 3*A* (*panels 2* and *3 versus 4*) and (*b*) labeled profiles in Fig. 3*C* (*panels 2* and *4*) to the unlabeled data in supplemental Fig. S1 (*black bars*). Moreover, immunodetectable incorporation of [^{33}P]orthophosphate into UGTs and PKCϵ confirmed both proteins are phosphorylated in parallel and that curcumin down-regulates the incorporation with eventual recovery without affecting specific protein, again suggesting PKCs support phosphorylation of UGT that is most likely regulated via signaling events.

UGT and PKC in the ER—To demonstrate co-localization of PKCϵ and ER-bound UGT1A7His, we first demonstrate the lack of overlapping background immunofluorescence. Because supplemental Fig. S3*B* (*panels 1*, *2*, and *4*) revealed no background immunofluorescence in non-transfected COS-1 cells with or without considering DAPI fluorescence (supplemental Fig. S3*B*, *panels 3* and *5*), we estab-

TABLE 1
Time course for curcumin glucuronidation in LS180 cells

HPLC eluate	Time (h)							
	0	0.25	1	2	3	6	12	24
					%			
Curcumin	100	98.5 ± 2.8	86 ± 3.0	82 ± 3.8	38 ± 3.5	34 ± 4.0	19.5 ± 2.9	1.3 ± 0.08
Curcumin glucuronides	0	1.5 ± 1.0	14 ± 2.0	19 ± 2.5	62 ± 4.2	66 ± 2.8	80.5 ± 4.2	98.7 ± 3.0

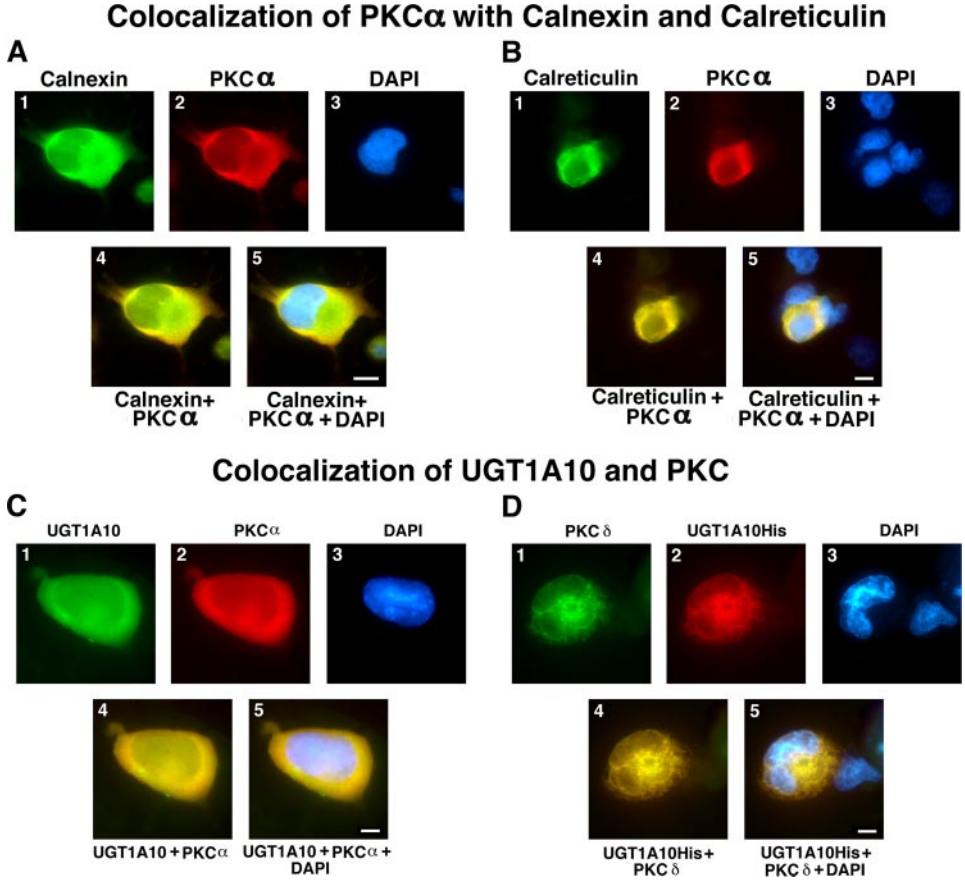

FIGURE 4. **Co-localization of PKCα with calnexin (*A*) or calreticulin (*B*) in control COS-1 cells.** Cells were processed for co-immunofluorescence as described under "Experimental Procedures." For calnexin and PKCα co-localization, calnexin was visualized with donkey anti-rabbit FITC conjugate, and PKCα was visualized with donkey anti-mouse TRITC conjugate. Assembly of fluorescence images (*panels 1* and *2*) indicates fusion-generated *yellow* immunofluorescence (*panel 4*) outside the nuclei (*panel 5*). For calreticulin and PKCα co-localization, calreticulin was detected with donkey anti-rabbit FITC conjugate, and PKCα was detected with donkey anti-mouse TRITC conjugate. Assembly of fluorescence images (*panels 1* and *2*) indicates fusion-generated *yellow* immunofluorescence (*panel 4*) outside the nuclei (*panel 5*). Co-localization of PKCα or PKCδ with UGT1A10His expressed in COS1 cells. Co-localization was determined by immunofluorescence that probed UGT1A10 with donkey anti-rabbit FITC conjugate and PKCα with donkey anti-mouse TRITC conjugate as described under "Experimental Procedures." *C*, assembly of fluorescence images (*panels 1* and *2*) indicates fusion, which generated *yellow* immunofluorescence (*panel 4*) outside the nuclei (*panel 5*). *D*, co-localization of PKC δ and UGT1A10His expressed in COS-1. Co-localization was analyzed by immunofluorescence with PKCδ detected with donkey anti-rabbit FITC conjugate, and UGT1A10His was detected with donkey anti-mouse TRITC as described under "Experimental Procedures." Assembly of fluorescence images (*panels 1* and *2*) merged to generate *yellow* fluorescence (*panel 4*) outside the nuclei as shown (*panel 5*). Background immunofluorescence images in non-transfected cells are shown in supplemental Fig. S4. *Scale bars* represent 20 μm (*A*) or 10 μm (*B–D*).

lished the fact that UGT1A7 and PKCϵ co-localize to the ER outside the nucleus. As shown in supplemental Fig. S3, we targeted phosphoserine-729-PKCϵ with rabbit anti-*phosphoserine*-729-PKCϵ with detection by donkey anti-rabbit FITC conjugate and UGT1A7His with mouse anti-His tag with detection by donkey anti-mouse TRITC conjugate; assembly of their fluorescence images fused to generate yellow fluorescence, confirming that *activated* PKCϵ (7) co-localizes with UGT1A7His (supplemental Fig. S3*A*, *panels 1*, *2*, and *4*) outside the nucleus according to DAPI fluorescence (supplemental Fig. S3*A*, *panels 3* and *5*).

Co-localization of PKCα with Calnexin and Calreticulin—Before continuing with PKC and UGT co-localization studies, we examined whether PKCα co-localizes with ER marker proteins. Although it is well documented that calnexin and calreticulin are ER marker proteins, it is not commonly appreciated that PKC isozymes localize or translocate to the ER membrane in response to appropriate signal(s) according to the Mochly-Rosen model discussed below (33). To assess co-localization of calnexin or calreticulin and PKCα in non-transfected COS-1 cells, rabbit anti-calnexin and mouse anti-PKCα were added as targets and visualized with donkey anti-rabbit FITC conjugate and donkey anti-mouse TRITC conjugate, respectively. To examine, separately, for co-localization of calreticulin and PKCα, rabbit anti-calreticulin and mouse anti-PKCα were added as targets and visualized with donkey anti-rabbit FITC conjugate and donkey anti-mouse TRITC conjugate, respectively. Through fusion of immunofluorescence images of calnexin and PKCα (Fig. 4*A*, *panels 1*, *2*, and *4*) and that for calreticulin and PKCα (Fig. 4*B*, *panels 1*, *2*, and *4*), it is evident that both ER markers co-localize with PKCα outside fluorescein-containing nuclei (Fig. 4, *A* and *B*, *panels 4* and *5*), which is consistent with our demonstrations showing that PKC isozymes co-localize with ER-bound UGT isozymes.

Co-localization of UGT1A10His and PKCα or -δ—To determine whether other PKC isozymes support UGT1A7 or UGT1A10, we carried out other co-localization studies. Because PKCα or PKCδ seldom co-immunoprecipitated with

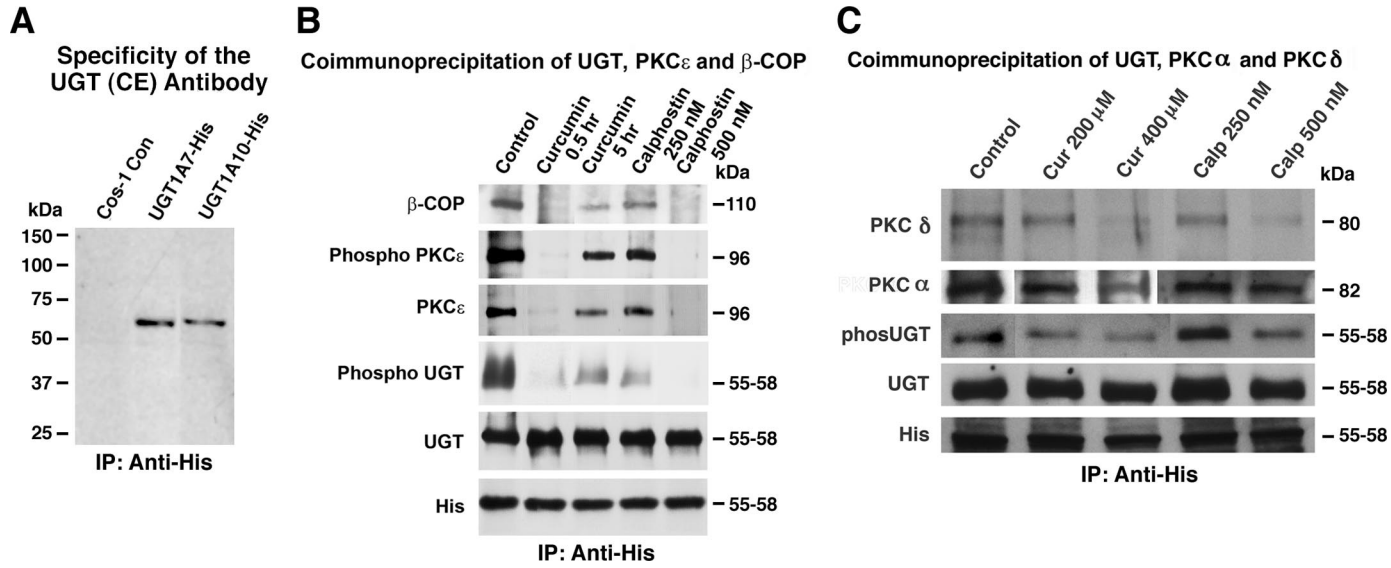

FIGURE 5. *A*, specificity of anti-UGT-CE. Non-transfected and UGT1A7His- and -1A10His-transfected COS-1 cells were processed for immunoprecipitation with anti-His as described under "Experimental Procedures." Western blots prepared after resolution of samples in a 4–15% SDS-PAGE system as described under "Experimental Procedures" were probed with anti-UGT-CE. *B*, co-immunoprecipitation of PKCε and UGT1A7His expressed in COS-1 cells. Upon terminating the experiment in which UGT1A7His-transfected COS-1 cells had been untreated or treated with 75 μM curcumin (as shown above) or calphostin-C for 1 h, 60,000 × *g* supernatants generated as described under "Experimental Procedures" were immunocomplexed with anti-His, trapped with protein A-Sepharose for resolution in a SDS-10% PAGE system, and transblotted onto a nitrocellulose membrane. Proteins migrated as follows: β-COP, 110 kDa; PKCε, 96 kDa; and UGT1A7His, 58 kDa. The membrane was probed according to "Experimental Procedures" with different primary antibodies as follows: β-COP (ε-RACK), phosphoserine-PKCε, PKCε, phosphoserine, UGT-CE, and His. *C*, co-immunoprecipitation of UGT1A10His, PKCα, and PKCδ. Co-immunoprecipitation of PKCα and PKCδ expressed in UGT1A10-transfeceted COS-1 cells, which had been treated 1 h each with curcumin or calphostin-C as shown, was carried out with 60,000 × *g* supernatants as described in the legend for *B*. Supernatants were immunocomplexed with anti-His, trapped with protein A-Sepharose for resolution in a 4 to 15% SDS-PAGE system, and transblotted onto a nitrocellulose membrane.

UGT1A7His, and PKCε seldom co-immunoprecipitated with UGT1A10 or 1A10His, we examined PKCα or PKCδ co-localization with 1A10 expressed in COS-1 cells. For PKCα and UGT1A10 co-localization, we exposed 1A10-transfected cells to mouse anti-PKCα, which was again visualized with donkey anti-mouse TRITC conjugate, and to rabbit anti-UGT-CE, which was visualized with donkey anti-rabbit-FITC conjugate (Fig. 4*C*, *panels 2* and *1*); assembly of the fluorescence images led to fusion that generated yellow fluorescence (*panel 4*) on a frequent basis, indicating the two proteins co-localized outside DAPI-fluorescent nuclei (*panel 5 versus 3*). For PKCδ and UGT1A10His co-localization, rabbit anti-PKCδ targeted PKCδ, which was visualized with donkey anti-rabbit FITC conjugate (Fig. 4*D*, *panel 1*), and mouse anti-His targeted 1A10His, which was visualized with donkey anti-mouse TRITC conjugate (*panel 2*); assembly of their fluorescence images generated yellow fluorescence (*panel 4*), which was evident outside DAPI-fluorescent nuclei (*panel 5 versus 3*). There was no detectable background cellular immunofluorescence for PKCα and UGT1A10 co-localization or for PKCδ and UGT1A10His co-localization (see supplemental Fig. S4, *A* and *B*). Thus, co-localization results suggest phosphorylation of UGT1A10 is most likely supported by PKCα and/or -δ, and not by PKCε, in COS-1 cells. Consistent with interactions with a different selection of PKCs, UGT1A10 appears in a substantially larger complex than UGT1A7 in preliminary purification studies.[4]

Specificity of the Anti-UGT-CE—To verify the specificity of anti-UGT-CE, we compared anti-His immunoprecipitates derived from non-transfected COS-1 cells *versus* those from UGT1A7His- and 1A10His-transfected COS-1 cells. Results show no detectable signal in non-transfected cells using anti-UGT-CE as shown in Fig. 5*A*, confirming our previous results (7).

Co-immunoprecipitation of PKCε, ε-RACK, and UGT1A7His from 1A7His-expressing COS-1 Cells—As we have clearly demonstrated that each of three PKC isozymes co-localizes with UGTs, we analyzed for the effect of curcumin and calphostin C on co-immunoprecipitation. Inasmuch as UGT1A7His and *phosphoserine*-729-PKCε co-localized in 1A7-transfected cells, we attempted to co-immunoprecipitate the two proteins with anti-His from solubilized cellular extracts (described under "Experimental Procedures") to analyze for related proteins by Western blot after resolution in a 10% SDS-PAGE system. For untreated cells, UGT protein, detected with anti-His and anti-UGT-CE (Fig. 5*B*, *panels 6* and *5*, *lane 1*), was heavily phosphorylated as detected with anti-phosphoserine (*panel 4*); in addition, PKCε (*panel 3*) with high phosphoserine content (*panel 2*) was readily immunodetected using anti-PKCε and anti-phosphoserine-729-PKCε, respectively. We also detected the receptor for *activated* PKCε (19), ε-RACK (β-COP) (*panel 1*), the ε-specific receptor that translocates/anchors *activated* PKCε proximal to its substrate. If one compares the effects of curcumin and calphostin-C treatment, 75 μM curcumin caused complete disassociation of β-COP and PKCε and dephosphorylation of UGT1A7 at 30 min with incomplete recovery by 5 h, whereas 250 nM calphostin-C caused minor effects on these same proteins, but 500 nM completely disassociated PKCε and β-COP and dephosphorylated

[4] N. K. Basu, R. Banerjee, and I. S. Owens, manuscript in preparation.

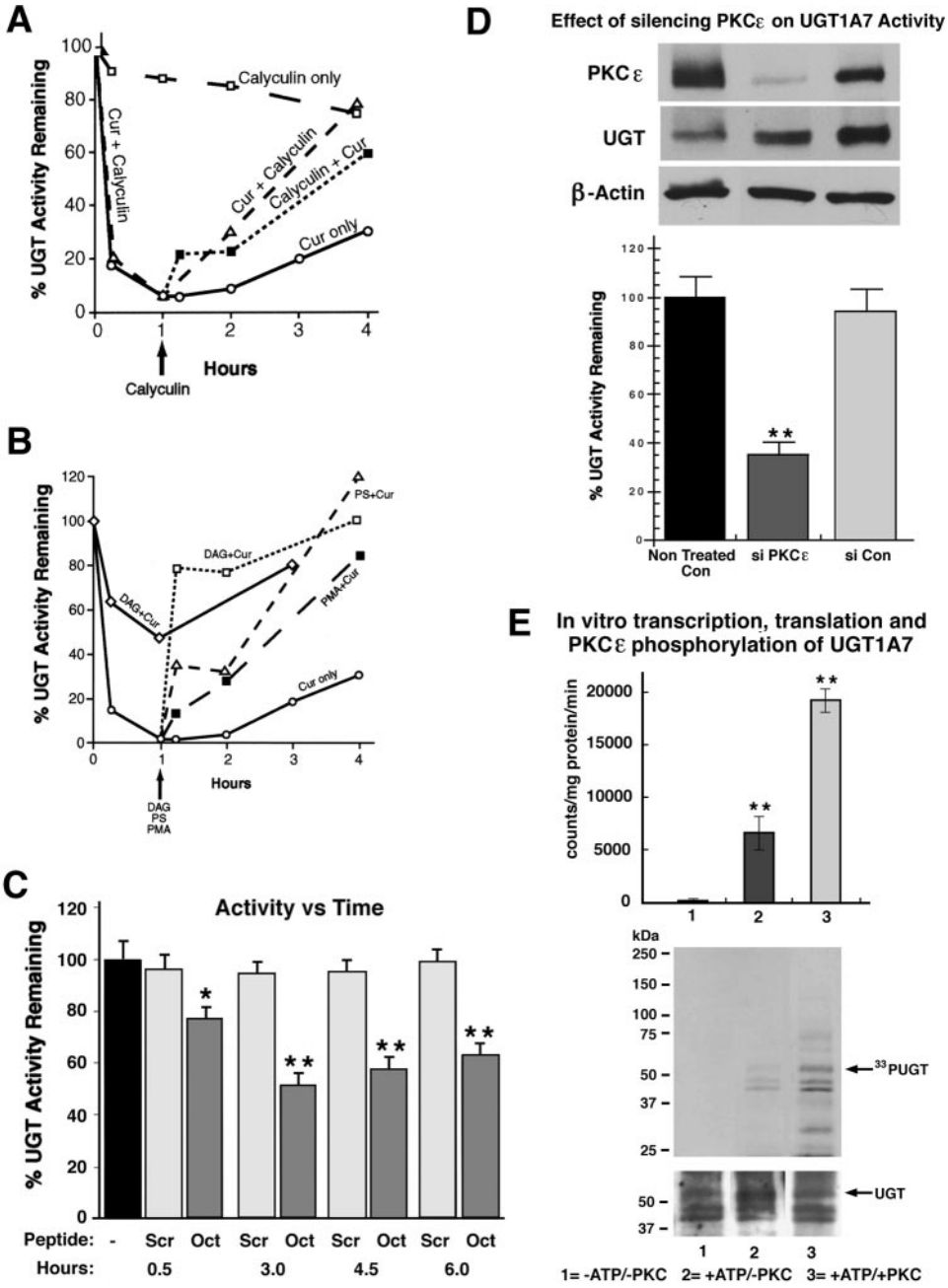

FIGURE 6. *A*, effect of calyculin-A on curcumin-inhibited UGT activity in LS180 cells. Calyculin-A (6 nM) was added with or without curcumin or 1 h after curcumin (50 μM); its effect on control or inhibited cells was assessed as shown. (Calyculin-A is a protein phosphatase 1 inhibitor.) Standard errors for UGT activity range between ± 1 and $\pm 4\%$ in three experiments performed in triplicates. *B*, effects of PKC agonists on curcumin (50 μM)-inhibited UGT were examined with either 30 μM DAG, 2.0 μM PMA, or 100 μg/ml PS as shown. Control activity was 1817 $\pm$ 88 pmol/mg of protein/h. Standard errors for UGT activity range between ± 2 and $\pm 5\%$ in three separate experiments. *C*, effect of PKCε-specific translocation inhibitor on UGT activity. Non-conjugated 8-amino acid peptide (Oct) (175 μM) or its scrambled (Scr) control was introduced into saponin-permeabilized (18) LS180 cells as described under "Experimental Procedures." Also, the rationale for PKC isozyme-specific inhibition is described under "Experimental Procedures" and/or "Results." Control activity was 1952 $\pm$ 102 pmol/mg of protein/h. UGT assays in *panels A–D* used capsaicin and eugenol (not shown). *, $p \leq 0.01$; **, $p \leq 0.001$. *D*, effect of silencing PKCε on UGT1A7 activity. siRNA specific for PKCε (100 nM) or control siRNA (100 nM) was transfected into COS-1 cells following expression of UGT1A7 for 24 h; incubation continued for 48 h before harvesting cells for glucuronidation of eugenol or mycophenolic acid as shown (see Ref. 51) in a 2-h incubation. For Western blot analysis, samples were solubilized and fractionated by centrifugation as previously described (7), and 60,000 $\times$ *g* supernatants were resolved in a 4 to 15% SDS-PAGE system and transblotted. For Western analysis, anti-PKCε, anti-UGT-CE, and anti-β-actin were used as previously described (7). *, $p \leq 0.01$; **, $p \leq 0.001$. *E*, *in vitro* transcription, translation, and phosphorylation of UGT1A7His by PKCε. pcDNA3.1-UGT1A7His construct was linearized and transcribed for synthesis of nascent protein to undergo *in vitro* PKCε-dependent phosphorylation using [γ-^{33}P]ATP with as described under "Experimental Procedures"; accordingly, aliquots of the kinased samples were counted. Affinity-purified control and experimental samples of [^{33}P]UGTHis were analyzed in duplicate gels. One was dried for autoradiography and one was used for Western blot with anti-UGT-CE as described under "Experimental Procedures." Samples are defined at the *bottom* of *E*. **, $p \leq 0.001$.

UGT1A7. The coordinate loss of PKCε, β-COP, and phosphorylation of UGT following curcumin or calphostin-C treatment indicates these factors are likely located in a complex to support UGT1A7 phosphorylation and activity. Consistent with these results, overexpression of PKCε increased UGT1A7 activity expressed in COS-1 cells (7). Interestingly, UGT1A7His required approximately one-half concentration compared with wild-type UGT1A7; hence, 75 μM curcumin for 1A7His is equivalent to 150 μM for UGT1A7 to achieve similar inhibitions (see Figs. 1*A*, S1, and 5*B*).

Co-immunoprecipitation of PKCα or PKCδ with UGT1A10His—Consistent with the co-localization results, PKCα or PKCδ is co-immunoprecipitable with UGT1A10His from solubilized cellular extracts when analyzed by Western blot following resolution in a 4 to 15% SDS-PAGE system (Fig. 5*C*). Whereas analysis with anti-His and anti-UGT-CE showed no effect on UGT1A10 protein level by treatments with 200 and 400 μM curcumin or 250 and 500 nM calphostin-C, both chemicals caused considerable loss of UGT1A10 phospho-content and of PKCα or PKCδ protein content. By comparison, however, there was far less loss of UGT1A10 phospho-content and of PKCα and PKCδ levels in this study with 200 μM curcumin and 500 nM calphostin C compared with the drastic effect of 75 μM curcumin and 500 nM calphostin-C on UGT1A7 and PKCε (compare with Fig. 5*B*), indicating UGT1A10 and PKCα/δ are much more resistant to these agents in the COS-1 cell model.

Evidence that the Phosphorylation Process of UGTs Participates in PKC-mediated Signaling—To determine whether UGT phosphorylation is regulated by PKC-dependent signaling, we examined the effects of various PKC agonists and antagonists on UGT activity in curcumin-inhibited LS180 cells. Addition of phosphatase inhibitor I, calyculin-A (34), at time zero *versus* its addition

1-h later (Fig. 6*A*, *arrow*) shows calyculin-A protected against curcumin inhibition at both times, but it was most effective when added at time zero, suggesting calyculin-A partially protected by inhibiting phosphatase removal of phosphates group(s). Also, 100 μM sodium orthovanadate showed 35–40% stimulation of constitutive UGT activity (data not shown). Dephostatin revealed minor protection against curcumin inhibition. The response to phosphatase treatment is consistent with phosphorylation that is undergoing regulation due to phosphatase (35) and kinase signaling events.

Our attempts to determine whether the PKC system involving UGT phosphorylation is mediated by the EGF receptor in colon cells showed a 20% increase in glucuronidating activity with EGF treatment (data not shown). Similarly, curcumin showed a 20% displacement of [^{125}I]EGF binding to its receptor. It was not possible, therefore, to show a highly significant involvement of EGF in UGT activity in LS180 cells.

Furthermore, we examined whether treatment of LS180 cells with typical PKC agonists, DAG, PMA, and PS, could stimulate curcumin-inhibited UGT, which was shown in Fig. 5*B* to be dissociated from PKCϵ (33). When 30 μM DAG and curcumin were combined, activity was only reduced 50% in 1 h (Fig. 6*B*) compared with nearly 100% with curcumin alone; its addition to inhibited cells (*arrow*) showed a robust 80% recovery that gradually reached 100% after 3 h. Similar treatment of inhibited UGT with PMA (2.0 μM) showed 80% recovery by 3 h, whereas PS initially showed 35% recovery that increased to 120%. By comparison, curcumin alone showed only 30% recovery by 3 h. Phosphorylation of UGTs regulated by PKC-mediated signaling is similar to that seen for other cellular processes following treatment with DAG, PMA, or PS, which leads to rapid activation with PKC usually undergoing attachment to membranes or other structures (36, 37) with increased phosphorylation of substrates.

Effects of PKCϵ-specific Translocation Agonist- and Antagonist-peptides on UGTs in LS180 Cells—Recently, it was determined that activated PKC isozymes are translocated or compartmentalized proximal to substrate by binding to an isozyme-specific receptor for activated C-kinase (RACK) (33, 38, 39) such that substrate specificity is, at least, partially imposed by differential localizations. Exposure of curcumin-inhibited cells to the pseudo-ϵ-RACK peptide agonist, which stimulates translocation of PKCϵ (38) in a concentration-dependent manner, culminated in 45% maximum curcumin inhibition of UGT after correction for Antennapedia carrier-conjugated control (supplemental Fig. S5). This was, predictably, due to increased PKCϵ binding to ϵ-RACK proximate to UGT with greater phosphorylation and glucuronidating activity (33). Because pseudo-ϵ-RACK and ϵ-RACK sites of PKCϵ bind intramolecularly to maintain the inactive state, pseudo-ϵ-RACK *peptide* competes out binding of pseudo-ϵ-RACK allowing the higher affinity ϵ-RACK translocator to displace, subsequently, the pseudo-specific peptide causing partial activation/translocation with PKCϵ anchorage near its substrate (36).

Because part of the ϵ-RACK binding site for translocation of PKCϵ is within its unique V1 segment (33, 40), we tested an appropriate peptide sequence from that region on constitutive UGT in LS180 cells. Addition of a translocation inhibitor octapeptide (Oct) caused 50% inhibition of UGT activity at 3 h compared with an insignificant effect by its scrambled (Scr) control (Fig. 6*C*). Previously, we showed that increasing concentrations of the Oct peptide attached to Antennapedia carrier (38) caused progressive inhibition culminating at 50% (without correction for activation) after 3 h (7), whereas carrier controls showed a consistent 20–30% increase in activity. Earlier studies concerned with PKCϵ- and -β-specific translocation inhibitor peptides showed, on average, 30–50% inhibition (41, 42), similar to our results. Based on the translocation model for *activated* PKCϵ that undergoes anchorage via ϵ-RACK (33) at sites proximal to its substrate, we conclude that PKCϵ and, most likely, PKCα are involved in phosphorylation of UGTs in LS180 cells. Moreover, actions of PKCϵ agonist and antagonist translocation-specific peptides (36, 39) on UGT activity provide strong evidence that PKCϵ can dissociate from its receptor causing breaks in signaling events, as well as UGT phosphorylation and glucuronidating activity in LS180 cells.

Effect of PKCϵ-specific siRNA on PKCϵ and UGT1A7 and Its Activity—To gain additional evidence that PKCϵ supports UGT1A7His activity, we tested the effect of targeted disruption of PKCϵ-specific mRNA on 1A7His expressed in COS-1 cells 48 h after treatment using Western blot analysis and *in vitro* activity. Results show that, whereas UGT1A7 protein level was not affected by PKCϵ-specific siRNA (Fig. 6*D*, *panel 2*), there was a 65% loss of its activity (*panel 4*), which is consistent with the nearly complete loss of detectable PKCϵ protein (*panel 1*) that predictably supports phosphorylation of UGT1A7 that is required for its activity.

In Vitro Transcription, Translation, and Phosphorylation of UGT1A7 by PKCϵ—To demonstrate unequivocally that PKCϵ phosphorylates UGT1A7, we carried out *in vitro* transcription and translation generating UGT1A7His for *in vitro* phosphorylation by PKCϵ. PKCϵ-dependent incorporation of [γ-^{33}P]ATP into nascent UGTIA7His was 2.7-fold higher than in the absence of the kinase (Fig. 6*E*). Affinity purification of the newly synthesized UGT1A7His phosphorylated by PKCϵ confirms UGT1A7 is a substrate (*middle panel*, *lane 3*) for this kinase when compared with unlabeled 1A7 in the absence of this isozyme (*middle panel*, *lane 2*). A Western blot probed with anti-UGT-CE (*bottom panel*) shows newly synthesized protein requires both ATP and PKCϵ for phosphorylation. It is noted that the molecular mass of nascent UGT1A7His is ~53 kDa (Fig. 6*E*, *middle* and *bottom panels*) compared with 55–58 kDa for in-cell synthesized UGT1A7His (Fig. 5, *A*–*C*).

Identification of Possible Constitutive PKC Activators That Support UGT Activity—Because routine cellular oxidants, also known as ROS, were suggested to modulate zinc-complexed thiols in the regulatory domain of PKC leading to activation (10, 43), and H_2O_2 was shown to activate PKC via increased phosphorylation of tyrosine in its catalytic domain (20, 21, 39), it was of interest to determine if these second messengers affected UGT activity. Because oxidants were used in both studies cited, we examined the effects of catalase and herbimycin-A on constitutive and H_2O_2-activated UGT in LS180 cells. Upon establishing optimum levels of catalase and herbimycin-A to down-regulate constitutive UGT (Fig. 7*A*) and conditions to H_2O_2-activate UGT and PKCϵ maximally (Fig. 7*B*, *lower*, *bar 5*),

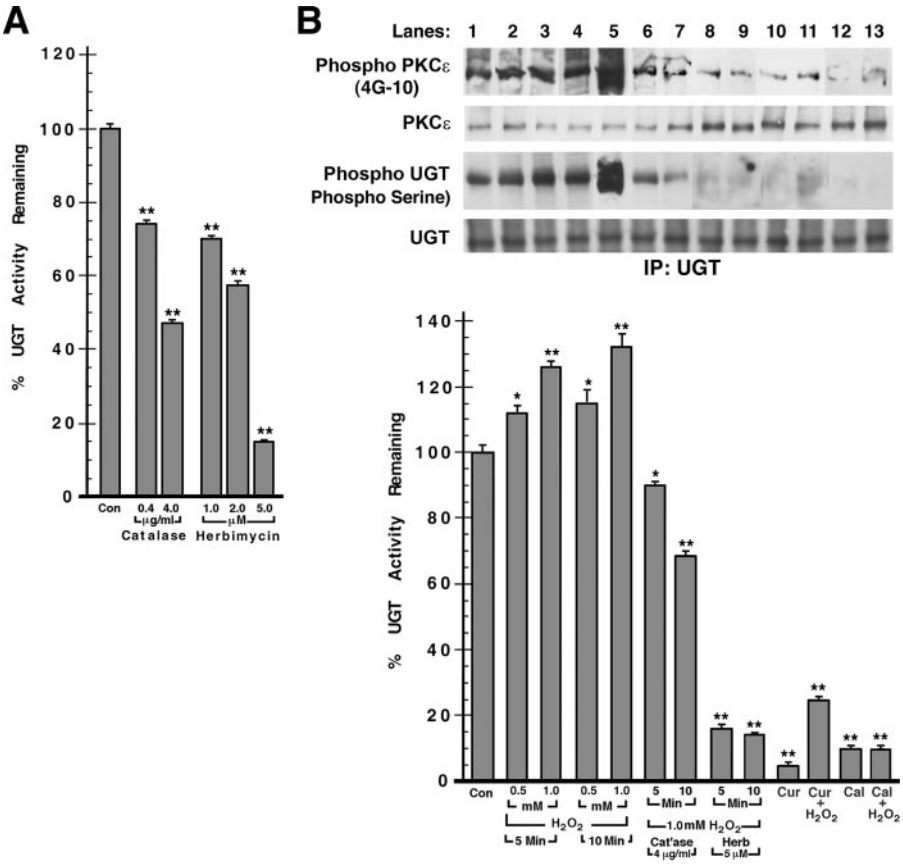

FIGURE 7. **Effects of ROS on UGT activity in LS180 cells.** *A*, control LS180 cells were treated with 0.4 and 4.0 μg/ml catalase for 40 min or with 1.0, 2.0, and 5.0 μM herbimycin-A for 40 min. *, $p \leq 0.01$; **, $p \leq 0.001$. *B*, cells were treated with 0.5 or 1.0 mM H_2O_2 for 5 and 10 min. Cells under *B* were preincubated with 4.0 μg/ml catalase (*Cat'ase*) or 5.0 μM herbimycin-A (*Herb*) for 30 min before the addition of 1.0 mM H_2O_2 for an additional 5 or 10 min. Cells were also treated with 50 μM curcumin for 30 min or 250 nM calphostin-C for 30 min before addition of 1.0 mM H_2O_2 for 10 min. UGT activity was measured with eugenol with control value 8431 $\pm$ 141 pmol/mg of protein/h. A similar profile was observed with capsaicin as substrate. *, $p \leq 0.01$; **, $p \leq 0.001$.

catalase (50%) and herbimycin-A (88%) treatments were shown to inhibit constitutive or H_2O_2-activated UGT equally (Fig. 7*A*, *bars 1* and *3 versus* Fig. 7*B*, *bars 5* and *7* and Fig. 7*A*, *bars 4* and *6 versus* Fig. 7*B*, *bars 5* and *9*). Hence, catalase was far less efficient in removing ROS than herbimycin-A was at inhibiting H_2O_2-activated tyrosine phosphorylation of PKCs. Hydrogen-peroxide treatment enhanced phosphotyrosine-PKCϵ and phosphoserine-UGT in parallel reaching a maximum simultaneous with that for UGT activity; following maximum H_2O_2 activation (Fig. 7*B*, *panels 1* and *3*), catalase- and herbimycin-A-dependent decreases in phosphotyrosine-PKCϵ and phosphoserine-UGT appeared to parallel decreases in UGT activity (Fig. 7*B*, compare *bars 5–7* with *5*, *8*, and *9*). Also, 50 μM curcumin nearly abolished phosphotyrosine-PKCϵ and phosphoserine-UGT with nearly complete inhibition of UGT activity (Fig. 7*B*, *panels 1* and *3*, *lane 10 versus bar 10*); H_2O_2 activation after curcumin treatment enhanced phosphotyrosine-PKCϵ and phosphoserine-UGT with a modest increase in UGT activity (*bar 11*), whereas calphostin-C treatment completely abolished phosphorylation of PKCϵ and UGT with no response to H_2O_2 treatment (*lanes 12* and *13* and *bars 12* and *13*). These observations suggest ROS-mediated activation of PKC is important in sustaining phosphorylation of UGT by PKC-dependent signaling. Further, UGT down-regulation by the tyrosine kinase-specific inhibitor, herbimycin-A, suggests cellular oxidant-/H_2O_2-activated PKC via tyrosine phosphorylation also plays a role in sustaining UGT activity (20, 21).

DISCUSSION

Overall, we have provided evidence that UGTs in LS180 cells and the 10 different human isozymes independently expressed in COS-1 cells undergo phosphorylation, which is supported by PKC isozymes based on inhibition of both UGT activity and its phosphorylation by curcumin or calphostin-C. (Our earlier studies uncovered three to five predicted PKC phosphorylation sites in each of 10 UGTs examined (5). Inhibition was confirmed with six different substrate activities tested (4, 6) with extracts of LS180 and transfected COS-1 cells. Mutants at two of four sites in recombinant UGT1A1 (5), UGT1A7 (7), and UGT1A10 (6, 7) had null activity, and activity for the mutant at the third site showed a marked shift in pH optimum for assay conditions with emergence of new substrate activities (7). The fourth site is predicted to be exposed to the cytoplasm (44) distal to the active site projecting into the ER lumen. Co-immunoprecipitation of PKCϵ, PKCα, and PKCδ with UGT1A7, UGT1A10, and UGT1A10, respectively, confirmed preferential association of select PKC and UGT isozymes. Our demonstration of greater resistance of UGT1A10 association with PKCα and -δ than UGT1A7 to PKCϵ is consistent with the higher concentration of curcumin and calphostin-C required to inhibit 1A10 than 1A7 activity. The fact that UGT1A10 required 2- to 2.5-times higher concentrations of curcumin and calphostin-C than 1A7 to achieve 95% inhibition suggests the PKCs and/or UGTs are differentially sensitive to the two reagents. Although the PKCϵ-specific siRNA (45) markedly reduced UGT1A7 activity, *in vitro* PKCϵ-dependent phosphorylation of newly synthesized UGT1A7His confirms that 1A7 serves as a *bona fide* substrate for the kinase. Thus, we provide strong evidence that at least three PKC isozymes are involved in phosphorylation of UGT isozymes. Moreover, our demonstration here that PKCα co-localizes with both ER-marker proteins, calnexin and calreticulin, is independent evidence that PKC isozymes attach to ER, which agrees with a previous demonstration that PKC and calreticulin are associated (46).

To understand UGT phosphorylation and its linkage to PKC, we examined properties associated with PKC control

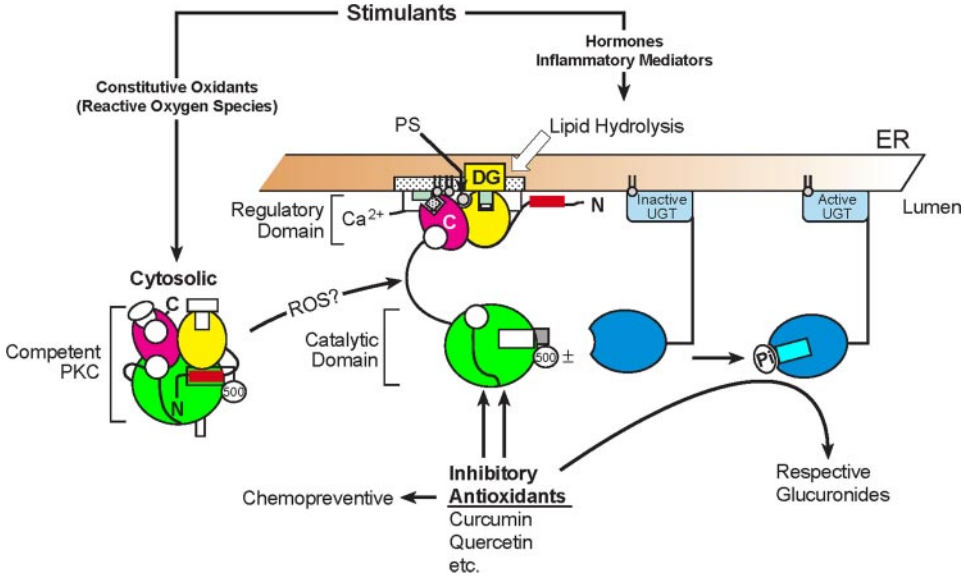

FIGURE 8. **Proposed model for effects of agonists and antagonists on PKC activity that controls UGT activity.** The PKC schematic illustrates two modes of regulation: 1) well-established upstream phosphoinositide-dependent kinase-1 and tyrosine kinase(s) phosphorylate conserved serine/threonine and tyrosines (20, 21, 36, 39), respectively, in the catalytic domain generating putative competent and active PKC, and 2) the allosteric long term mediator (PMA) or lipid-derived short term agonists, DAG and PS (Fig. 6*B*), activate competent PKC via the regulatory domain (36) triggering attachment to specific cellular structures. Although the schematic suggests direct phosphorylation of ER-bound UGT by PKC based on parallel curcumin/calphostin-C inhibition of phosphoserine/radiolabeling with [^{33}P]orthophosphate and UGT activity (Fig. 3, *A–C*), the fact that UGT1A7 acquired new substrate activity due to loss of serine 432 phosphorylation by PKCϵ translocation inhibitor peptide strongly suggests that PKCϵ directly phosphorylates UGT1A7 (7). Curcumin or calphostin-C inhibits attachment of PKC to molecular structures (7, 33, 36) (Fig. 5, *B* and *C*). Further, cellular oxidants and ROS can activate PKC via disruption of oxygen-sensitive zinc-complexed cysteine thiols in the regulatory domain (10, 47) and/or via stimulation of tyrosine phosphorylation of PKC (Fig. 7*B*). Consistent with PKC activation via H_2O_2-stimulated tyrosine phosphorylation, which is inhibited by herbimycin-A (20, 21), we observed inhibition of both constitutive and peroxide-stimulated UGT by both agents (Fig. 7, *A* and *B*). Inasmuch as cellular exposure to high concentrations of oxidized antioxidants, such as curcumin and nordihydroguaiaretic acid (4), can disrupt critical cysteines in the catalytic domain (10, 43, 47), the inhibitory effects of 50 μM curcumin, but not 25 μM (not shown), on both PKC phosphorylation and UGT activity are consistent with curcumin antioxidant action. Low levels (1.0–10 μM) of antioxidant polyphenols can act chemopreventively to scavenge oxidants (52). Potentially, UGTs with high K_m values ($\geq$10 μM) (4) and PKC isozymes with differential inhibitory sensitivities (Fig. 2) to polyphenols enable the PKC-UGT signaling pathway to adapt to different conditions and remain functional to beneficial chemopreventive action.

of cellular events such as proliferation, apoptosis, adhesion, stress, and others (36). PKCϵ and -δ are among the DAG-dependent novel category (δ, ϵ, η, and θ), and PKCα is among the DAG- and calcium-dependent classic category (α, βI, βII, and γ), indicating both categories are involved in controlling UGT activity in colon and COS-1 cells. In addition, protection against curcumin inhibition of UGT phosphorylation by phosphatase inhibitor, calyculin-A, effectively restores PKC phosphorylation, thereby providing evidence that one or more phosphatases participate in regulating UGT phosphorylation and activity. The robust stimulatory effects of typical PKC-dependent signaling mediators (37), DAG, PMA, and PS, on curcumin-inhibited UGT indicate that phosphorylation undergoes regulation via signaling events. Our failure to observe these agonist(s) effects on constitutive UGT activity in control LS180 cells suggests signaling conditions are maximally optimized. Consistent with other PKC-mediated phosphorylation models (33), modulations of UGT activity by antagonist and agonist translocation-specific peptides for PKCϵ (7, 33, 38, 40, 41) are evidence that UGT phosphorylation supported by PKC is regulated similar to that observed in other cellular models.

To identify constitutive PKC activators that support UGT activity, we considered the potential for routine endogenously generated superoxide anions (20, 21) to activate PKCs by disrupting oxygen-sensitive zinc-complexed thiols in the regulatory domain of PKC (10) and/or by stimulating tyrosine phosphorylation in the catalytic domain, which is sensitive to herbimycin-A (20, 21) (Fig. 7). Concentration-dependent catalase and herbimycin-A-based decreases in constitutive UGT activity in LS180 cells was essentially duplicated with H_2O_2-activated UGT activity. For example, catalase and herbimycin down-regulation of UGT was independent of cellular conditions, which suggests that constitutive oxidants or ROS may, in fact, act as second messengers to activate PKCs via effects on both the regulatory domain and tyrosine phosphorylation in the catalytic domain to sustain constitutive UGT phosphorylation (Fig. 7*B*). Hence, rapid down-regulation of constitutive UGT activity by antioxidant, curcumin, is consistent with oxidants or ROS stimulants to sustain activity, as depicted in Fig. 8.

A credible rationale for why UGTs serve as targets for the PKC-mediated signaling pathway may relate to effects that naturally occurring chemicals, some of which are UGT substrates, have on the unique structural features of thiols in PKC regulatory domain (10, 43). In addition, it is noted that H_2O_2-responsive tyrosine phosphorylation sites exist in the catalytic domain (20, 21) and antioxidant-inhibitable thiols exist in the catalytic domain (10, 47). Oxidation of cysteines in the regulatory region by cellular oxidants releasing autoinhibition with cofactor-independent activation of PKC (10, 20, 21), and inhibition by high levels of oxidized antioxidants acting on critical cysteines in the catalytic domain (10, 43, 47) make the isozymes targets (10, 47). Whereas routine cellular oxidants capable of providing on-going activation of PKCs (21–23) to support serine/threonine-based phosphorylation of critical constitutive enzymes, UGTs, which have a vast capacity to inactivate agents detrimental to PKCs, could represent the interdependent pressure for the enzymes described in this report. Predictably, a balance in oxidants and antioxidants is critical for the homeostasis of PKC activity, as well as induced and episodic activation of PKCs, to allow optimal regulation of the many cellular functions controlled by this kinase system. Constitutive UGTs have the capacity to glucuronidate diet-derived inhibitory polyphenolic antioxidants (48) to prevent cel-

lular accumulation and reduce the threat to homeostasis of PKC functions. Examples of such antioxidants are curcumin, quercetin, and nordihydroguaiaretic acid (Fig. 1*B* and Ref. 4).

Although it is indicated that cells need and use signal transduction to detect and respond appropriately to a changing environment (49), finding the active state of UGT isozymes is controlled by signaling events suggests protecting the cell against chemical exposure necessarily represents a changing environment to which the cell must respond with appropriate modifications (49). UGT conversion of a vast number of chemicals to high excretability that is linked to signal-regulated phosphorylation suggests glucuronidation represents an adaptable response that is sustained under many conditions. The role phospho-group(s) play in UGT catalysis has not been established. The fact that our earlier report (Fig. 5 in Ref. 7) indicated the UGT1A7-S432G mutant at a PKC phosphorylation site or targeted PKCϵ-specific inhibition of 1A7-expressed in COS-1 cells gained new substrates signifies that one or more phosphogroups participate in substrate selection. Based on this result, it is possible that regulated phosphorylation via signaling allows UGT adaptations of differential phosphate utilization to convert (inactivate) the numerous chemical structures that an isozyme handles. Moreover, this is the first demonstration, to our knowledge, that PKC mediates regulated phosphorylation of ER-bound drug-metabolizing enzymes.

The dual capacities of chemopreventive agents to be beneficial antioxidants and, at the same time, serve as UGT substrates are possible (Fig. 8). Beneficial antioxidant effects are reported to occur at relatively low concentrations, ranging from 1.0 to 10.0 μM, for many chemopreventive polyphenols (28, 50). By comparison, efficient metabolism of exogenous chemicals by UGTs, which generally have K_m values >10 μM (4), is predicted to occur at relatively high concentrations. Less than inhibitory levels allow both PKC and UGT activity (28), and, by inference, constitutive PKC and UGT activities appear interdependent, which could be critical for proper PKC-mediated signaling.

A complete understanding of the dependence of UGT activity on PKC under various cellular conditions should become clearer in the future. Finding that this primary detoxification system, which is also gastrointestinally distributed (4), is subject to rapid down-regulation by dietary and other antioxidants demonstrates the presence of an unsuspecting risk of facilitated absorption of toxins and/or therapeutic drug levels due to rapid down-regulation of UGT isozymes. Importantly, the dramatic and transitory down-regulation of UGT by agents that target PKC has significant *in vivo* implications for establishing models for blocking glucuronidation so as to greatly improve absorption and therapeutic efficacy of glucuronidatable drugs (51) and to make appropriate determinations about chemical toxicities, therapeutic drug administrations, and other PKC-dependent cellular events.

Acknowledgment—We thank Dr. Tapas Saha for providing technical assistance with siRNA transfections and immunofluorescence.

REFERENCES

1. Dutton, G. J. (1980) in *Glucuronidation of Drugs and Other Compounds* (Dutton, G. J., ed) pp. 69–78, CRC Press, Boca Raton, FL
2. Ritter, J. K., Crawford, J. M., and Owens, I. S. (1991) *J. Biol. Chem.* **266,** 1043–1047
3. Wells, P. G., Mackenzie, P. I., Chowdhury, J. R., Guillemette, C., Gregory, P. A., Ishii, Y., Hansen, A. J., Kessler, F. K., Kim, P. M., Chowdhury, N. R., and Ritter, J. K. (2004) *Drug Metab. Dispos.* **32,** 281–290
4. Basu, N. K., Ciotti, M., Hwang, M. S., Kole, L., Mitra, P. S., Cho, J. W., and Owens, I. S. (2004) *J. Biol. Chem.* **279,** 1429–1441
5. Basu, N. K., Kole, L., and Owens, I. S. (2003) *Biochem. Biophys. Res. Commun.* **303,** 98–104
6. Basu, N. K., Kubota, S., Meselhy, M. R., Ciotti, M., Chowdhury, B., Hartori, M., and Owens, I. S. (2004) *J. Biol. Chem.* **279,** 28320–28329
7. Basu, N. K., Kovarova, M., Garza, A., Kubota, S., Saha, T., Mitra, P. S., Banerjee, R., Rivera, J., and Owens, I. S. (2005) *Proc. Natl. Acad. Sci., U. S. A.* **102,** 6285–6290
8. Lang, D. R., and Racker, E. (1974) *Biochim. Biophys. Acta* **333,** 180–186
9. Kellis, J. T., and Vickery, L. E. (1984) *Science* **225,** 1032–1034
10. Gopalakrishna, R., and Jaken, S. (2000) *Free Radic. Biol. Med.* **28,** 1349–1361
11. Ciotti, M., Basu, N., Brangi, M., and Owens, I. S. (1999) *Biochem. Biophys. Res. Commun.* **260,** 199–202
12. Ritter, J. K., Sheen, Y. Y., and Owens, I. S. (1990) *J. Biol. Chem.* **265,** 7900–7906
13. Ciotti, M., Marone, A., Potter, C., and Owens, I. S. (1997) *Pharmacogenetics* **7,** 485–495
14. Chen, F., Ritter, J. K., Wang, M. G., McBride, O. W. Lubet, R. A., and Owens, I. S. (1993) *Biochemistry* **32,** 10648–10657
15. Ciotti, M., and Owens, I. S. (1996) *Biochemistry* **35,** 10119–10124
16. Ritter, J. K., Yeatman, M. T., Kaiser, C., Gridelli, B., and Owens, I. S. (1993) *J. Biol. Chem.* **268,** 23573–23579
17. Akhand, A. A., Pu, M., Senga, T., Kato, M., Suzuki, H., Miyata, T., Hamaguchi, M., and Nakashima, I. (1999) *J. Biol. Chem.* **274,** 25821–25826
18. Johnson, J. A., Gray, M. O., Karliner, J. S., Chen, C.-H., and Mochly-Rosen, D. (1996) *Circ. Res.* **79,** 1086–1099
19. Csukai, M., Chen, C.-H., De Matteis, M. A., and Mochly-Rosen, D. (1997) *J. Biol. Chem.* **272,** 29200–29206
20. Konishi, H., Tanaka, M., Takemura, Y., Matsuzaki, H., Ono, Y., Kikkawa, U., and Nishizuka, Y. (1997) *Proc. Natl. Acad. Sci. U. S. A.* **94,** 11233–11237
21. Min, D. S., Kim, E.-G., and Exton, J. H. (1998) *J. Biol. Chem.* **273,** 29986–29994
22. Sundaresan, M., Yu, Z., Farrans, V. J., Irani, K., and Finkel, T. (1995) *Science* **270,** 296–299
23. Suzuki, Y. J., Forman, H. J., and Sevanian, A. (1997) *Free Radic. Biol. Med.* **22,** 269–285
24. Surh, Y.-J. (2002) *Food Chem. Toxicol.* **40,** 1091–1097
25. Zhang, F., Altorki, N. K., Mestre, J. R., Subbaramaiah, K., and Dannenberg, A. J. (1999) *Carcinogenesis* **20,** 445–451
26. Rao, C. V., Rivenson, A., Simi, B., and Reddy, B. S. (1995) *Cancer Res.* **55,** 259–266
27. Hsu, H.-Y., and Wen, M.-H. (2002) *J. Biol. Chem.* **277,** 22131–22139
28. Chen, H.-W., and Huang, H.-C. (1998) *Br. J. Pharmacol.* **124,** 1029–1040
29. Larsen, E. C., Digennaro, J. A., Saito, N., Mehta, S., Loegering, D. J., Mazurkiewicz, J. E., and Lennartz, M. R. (2000) *J. Immunol.* **165,** 2809–2817
30. Pan, M.-H., Huang, T.-M., and Lin, J.-K. (1999) *Drug Metab. Dispos.* **27,** 486–494
31. Jobin, C., Bradham, C. A., Russo, M. P., Juma, B., Narula, A. S., Brenner, D. A., and Sartor, R. B. (1999) *J. Immunol.* **163,** 3473–3483
32. Fournès, B., Sadekova, S., Turbide, C., Létourneau, S., and Beauchemin, N. (2001) *Oncogene* **20,** 219–230
33. Mochly-Rosen, D. (1995) *Science* **268,** 247–251
34. Armstrong, S. C., Gao, W., Lane, J. R., and Ganote, C. E. (1998) *J. Mol. Cell Cardiol.* **30,** 61–73
35. Harmala-Brasken, A. S., Mikhailov, A., Soderstrom, T. S., Meinander, A., Holmstrom, T. H., Damuni, Z., and Eriksson, J. E. (2003) *Oncogene* **22,** 7677–7686
36. Dempsey, E. C., Newton, A. C., Mochly-Rosen, D., Fields, A. P., Reyland,

P. A., Insel, M. E., and Messing, R. O. (2000) *Am. J. Physiol.* **279,** 1429–1438
37. Karin, M. (1998) *Ann. N. Y. Acad. Sci.* **851,** 139–146
38. Dorn II, G. W., Souroujon, M. C., Liron, T., Chen, C.-H., Gray, M. O., Zhou, H.-Z., Csukai, M., Wu, G., Lorenz, J. N., and Mochly-Rosen, D. (1999) *Proc. Natl. Acad. Sci. U. S. A.* **96,** 12798–12803
39. Ron, D., and Kazanietz, M. G. (1999) *FASEB J.* **13,** 1658–1676
40. Johnson, J. A., Gray, M. O., Chen, C.-H., and Mochly-Rosen, D. (1996) *J. Biol. Chem.* **271,** 24962–24966
41. Yedovitzky, M., Mochly-Rosen, D., Johnson, J. A., Gray, M. O., Ron, D., Abramovitch, E., Cerasi, E. M., and Nesher, R. (1997) *J. Biol. Chem.* **272,** 1417–1420
42. Gray, M. O., Karliner, J. S., and Mochly-Rosen, D. (1997) *J. Biol. Chem.* **272,** 30945–30951
43. Maret, W., and Vallee, B. L. (1998) *Proc. Natl. Acad. Sci. U. S. A.* **95,** 3483–3488
44. Meech, R., and Mackenzie, P. I. (1997) *Clin. Exp. Pharmacol. Physiol.* **24,** 907–915
45. Pan, Q., Bao, L. W., Teknos, T. N., and Merajver, S. D. (2006) *Cancer Res.* **66,** 9379–9384
46. Rendón-Huerta, E., Mendoza-Hernández, G., and Robles-Flores, M. (1999) *Biochem. J.* **344,** 469–475
47. Gopalakrishna, R., and Gundimeda, U. (2002) *J. Nutr.* **132,** 3819S–3823S
48. Kühnau, J. (1976) *World Rev. Nutr. Diet.* **24,** 117–191
49. Moore, M. J., Kanter, J. R., Jones, K. C., and Taylor, S. S. (2002) *J. Biol. Chem.* **277,** 47878–47884
50. Bastianetto, S., Zheng, W.-H., and Quirion, R. (2000) *Br. J. Pharmacol.* **131,** 711–720
51. Basu, N. K., Kole, L., Basu, M., McDonaugh, A. F., and Owens, I. S. (2007) *Biochem. Biophys. Res. Commun.* **360,** 7–13
52. Ricciarelli, R., Tasinato, A., Clement, S., Özer, N. K., Boscoboinik, D., and Azzi, A. (1998) *Biochem. J.* **334,** 243–249